

“EXTRACTING BOREHOLE STRAIN PRECURSORS ASSOCIATED WITH THE LUSHAN EARTHQUAKE THROUGH PRINCIPAL COMPONENT ANALYSIS”

Kaiguang Zhu^{1,*}, Chengquan Chi¹, Zining Yu¹, Weichen Zhang¹, Mengxuan Fan¹, Kaiyan Li¹, Qiong Zhang¹

⁽¹⁾ Key Laboratory of Geo-Exploration Instrumentation, Ministry of Education, Jilin University, Changchun, China

Article history

Received January 23, 2018; accepted June 27, 2018.

Subject classification:

Borehole strain; Lushan earthquake; Principal component analysis; Eigenvalue and eigenvector; Earthquake precursor.

ABSTRACT

A YRY-4 borehole strainmeter installed at the Guza Station recorded anomalous changes in borehole strain data preceding the Lushan earthquake on April 20, 2013 (UTC) ($M_w = 7.0$). To identify earthquake-induced abnormal strain changes, we apply principal component analysis (PCA) for the first time to analyse the borehole strain data from the Guza Station. The first principal component eigenvalues and eigenvectors demonstrate that the anomalous days are mainly concentrated within two time periods: 1) October 25–December 30, 2012, and 2) April 15–19, 2013. A combined eigenvalue and eigenvector analysis reveals that the abnormal days exhibit a clustered distribution that is aggregated in the same location for both periods, intuitively indicating that there is a forceful correlation between the two anomalies. We tentatively infer that a similar process contributed to the formation of both anomalies and that these two anomalies are both earthquake precursors associated with the Lushan earthquake. These findings also indicate that the PCA approach exhibits potential for the extraction of earthquake precursor anomalies.

1. INTRODUCTION

Borehole strainmeters that are installed deeply into bedrock are capable of recording both continuous stress and continuous strain measurements and have consequently become an important tool for monitoring crustal deformation. High-resolution records from borehole strainmeters allow for the detection of subtle strain variations. Borehole strain data have been used to research various phenomena, including slow earthquakes [Sacks et al., 1978, 1981; Linde et al., 1996; Liu et al., 2009], seismic strain steps [McGarr et al., 1982; Asai et al., 2005; Qiu et al., 2003, 2004, 2015; Barbour et al., 2012], and volcanic eruptions [Voight et al., 2006; Hautmann et al., 2013; Sturkell et al., 2013].

The high-resolution records from borehole strain-

meters also provide the opportunity to investigate strain changes prior to earthquakes. Johnston et al. [1994, 2006] studied two large earthquakes in California with high-resolution continuous strain data. Qiu et al. [1998] found that the Douhe and Zhaogezhuang stress-monitoring stations that are located along a supposed fault zone observed significant tensile pulses of ground stresses normal to the fault zone before the great M7.8 Tangshan, China, earthquake in 1976, and they considered such surficial observations to reflect movements of the crust associated with earthquakes. Using data from the beginning of May 2008, Ouyang et al. [2009] observed that five RZB borehole strainmeters situated in the Chongqing section of the Three Gorges Reservoir region located 400–500 km southeast of the Wenchuan earthquake epicenter, simultaneously recorded corre-

lated anomalies, including a slow earthquake, a high rate of compressional strain, and high-frequency vibration and strain transients, which were relatively coherent at all of the sites.

Borehole strain data are affected by several other factors, and various data processing methods, such as wavelet analysis [Qiu et al., 2011], time-frequency spectrum analysis [Qi et al., 2011], and statistical analysis, are needed to clarify the association of such strain signals with crustal activity by revealing the characteristics of the subsurface physical mechanisms that are involved in strain change processes. Principal component analysis (PCA) is a statistical method that is widely employed to reveal relevant information in confusing datasets [Gómez et al., 2005]. PCA, which is a non-parametric method that does not utilize deviations from previously described strain changes to determine data anomalies, has the potential to describe the spatial distribution of earthquake-related strain changes. This method has been successfully applied during previous research, for many types of earthquake precursor data to obtain meaningful results. Gotoh et al. [2003] and Hattori et al. [2004, 2013] found that eigenvalues and eigenvectors are likely to be correlated with large earthquakes by using PCA to investigate ultra-low frequency (ULF) geomagnetic data. Similarly, Telesca et al. [2004] discovered earthquake precursor patterns in the daily variations of the principal components of eigenvalues by using PCA to investigate ULF geoelectrical data. Furthermore, Lin [2011] used PCA and image processing to identify ionospheric total electron content anomalies before a strong earthquake. C. Goltz [2001] used PCA to study the seismicity of the Southern California area and discussed the promising results in view of their implications, potential applications and possible precursory qualities. Fang Y et al. [2015] identified possible short- and medium-term earthquake precursors before the Lushan earthquake by using PCA to investigate the cross-fault data.

In this work, we apply PCA for the first time to time-series borehole strain data that were recorded at the Guza Station. The aim of this study is to detect anomalies in the borehole strain that preceded the Lushan earthquake and to investigate any correlation among the anomalies.

2. OBSERVATION AND DATA

At 08:02 on April 20, 2013, a Ms 7.0 earthquake occurred in Lushan County, Ya'an, Sichuan. The epicentre was located at 30.277° N and 102.937° E. According to the data published by the China Earthquake Networks

Center of the China Earthquake Administration, the earthquake magnitude was Ms 7.0 and the focal depth was approximately 13 km. The Lushan earthquake is a high-angle thrust event [Zeng X. F. et al., 2013]. The Guza Station is located at the southwestern extent of the Longmenshan fault zone. At the Guza station, the deformation observation instrumentation includes a very-long-period vertical pendulum tiltmeter, YRY-4 borehole strainmeter, DSQ water pipe inclinometer, SS-Y body piercing extensometer, and DZW digitalized gravity meter. The YRY-4 borehole strainmeter was installed in October 2006. Continuous recordings have been collected from this strainmeter at a sampling rate of one sample per minute since December 1, 2006. A seasonal change rule can clearly be seen in the strain data. Therefore, the borehole strain data from the Guza Station have a normal background [Qiu et al., 2011].



FIGURE 1. A location map showing the Guza Station and the Lushan earthquake epicentre.

The distance between the epicentre of the Lushan earthquake and the receiver at Guza Station is 72 km (Figure 1). The Lushan earthquake had a wide range of influence, and the physical phenomena taking place during earthquake preparation is very complicated, consequently we cannot exclude a-priori the possibility that the YRY-4 borehole strainmeter installed at the Guza Station recorded the strain anomaly phenomena taking place during earthquake preparation.

The YRY-4 borehole strainmeter contains four horizontally emplaced sensors to measure changes in the borehole diameter. The orientations of the four sensors are arranged at 45-degree intervals within a cylindrical case. With one additional measurement, a simple relationship among the four measurements can be obtained straight forwardly using the equation: $S_1 + S_3 = S_2 + S_4$.

, which is the self-consistency equation of the YRY-4 borehole strainmeter. This equation can be employed to estimate the credibility of the data. There are only

three independent variables under plain strain conditions at or near the Earth's surface. We can therefore derive various strains from the Guza recordings. The formulas used are as follows:

$$\begin{cases} S_{13} = S_1 - S_3 \\ S_{24} = S_2 - S_4 \\ S_a = (S_1 + S_2 + S_3 + S_4) / 2 \end{cases} \quad (1)$$

where S_a represents the areal strain, S_{13} and S_{24} and represent the two independent shear strains [Qiu et al., 2013a].

3. METHODOLOGY

3.1 PRINCIPAL COMPONENT ANALYSIS

PCA is a widely used technique in data analysis. It is computationally inexpensive, it can be applied to ordered and unordered attributes, and it can handle both sparse data and skewed data. PCA is a non-parametric method that is capable of extracting relevant information from complex data sets [Gómez et al., 2005], and it often reveals relationships that were not previously suspected, thereby allowing for an otherwise unordinary interpretation.

Mathematically the data are presented in a matrix Y of m rows and n columns:

$$Y = \begin{bmatrix} x_{11} & \cdots & x_{1n} \\ \vdots & \ddots & \vdots \\ x_{m1} & \cdots & x_{mn} \end{bmatrix} \quad (2)$$

where m is the number of samples, and n is the dimension of the sample.

First, we calculate the co-variance matrix $C_Y(m \times m)$ of the dataset $Y(m \times n)$, and the element y_{pq} in the co-variance matrix $C_Y(m \times m)$ can be calculated using the following formula:

$$y_{pq} = [1 / (N - 1)] \sum_{i=1}^N (x_p^i - \bar{X}_p)(x_q^i - \bar{X}_q) \quad (3)$$

where x_p^i and x_q^i are the p th and q th columns of the i th row of data, respectively, and \bar{X}_p and \bar{X}_q are the averages of the p th and q th columns of data, respectively. Here N is the number of samples.

We perform the eigenvalue decomposition using the co-variance matrix:

$$C_Y = \Lambda V V^T \quad (4)$$

where Λ is the eigenvalue matrix with $\lambda_1, \lambda_2, \dots, \lambda_m (\lambda_1 > \lambda_2 > \dots > \lambda_m)$ and V is the eigenvector matrix whose columns are v_1, v_2, \dots, v_m . The first principal

component eigenvalue and eigenvector are λ_1 and v_1 , respectively, which represent the principal characteristics of the signals. In this paper, the variations in the eigenvalue and eigenvector of the first principal component are investigated.

The obtained eigenvector has three dimensions in the vector space because the number of PCA dimensions is three, and it is a unit vector. To present the changes in the eigenvector more intuitively, we transform the eigenvectors to the unit spherical coordinate system, as shown in Figure 2. The eigenvector can be represented by θ and ϕ exclusively.

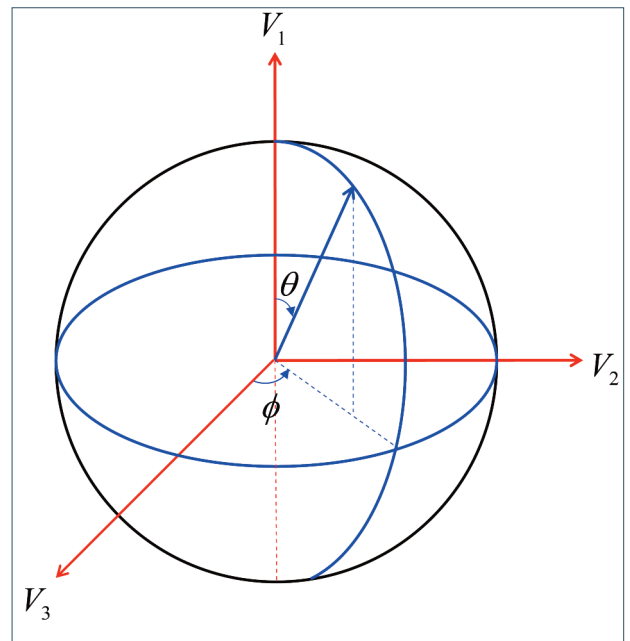


FIGURE 2. The unit spherical coordinate system of eigenvectors.

3.2 SYNTHETIC DATA

In order to verify the ability of PCA to extract this signal, we perform PCA on a synthetic data:

Firstly, we use suspected precursory anomaly signals and coseismic signal to construct synthetic signals, and the signal of the standard day is replaced by the Gauss signal. The synthetic signals are shown in Figure 3, the second and fifth days are precursory abnormal signals (in black box), and the eighth day is the coseismic signal (in red box).

Next, we perform PCA on the data matrix $X = [X_{13}, X_{24}, X_a]^T$. Figure 4 shows the covariance matrices of the standard days and the anomalous days. The covariance matrices of the precursory anomaly signals show the similar distribution, and with a large amplitude.

As is shown in Figure 5, eigenvalues and eigenvectors effectively detect anomalies signals. And eigenvectors show a similar distribution in the precursory

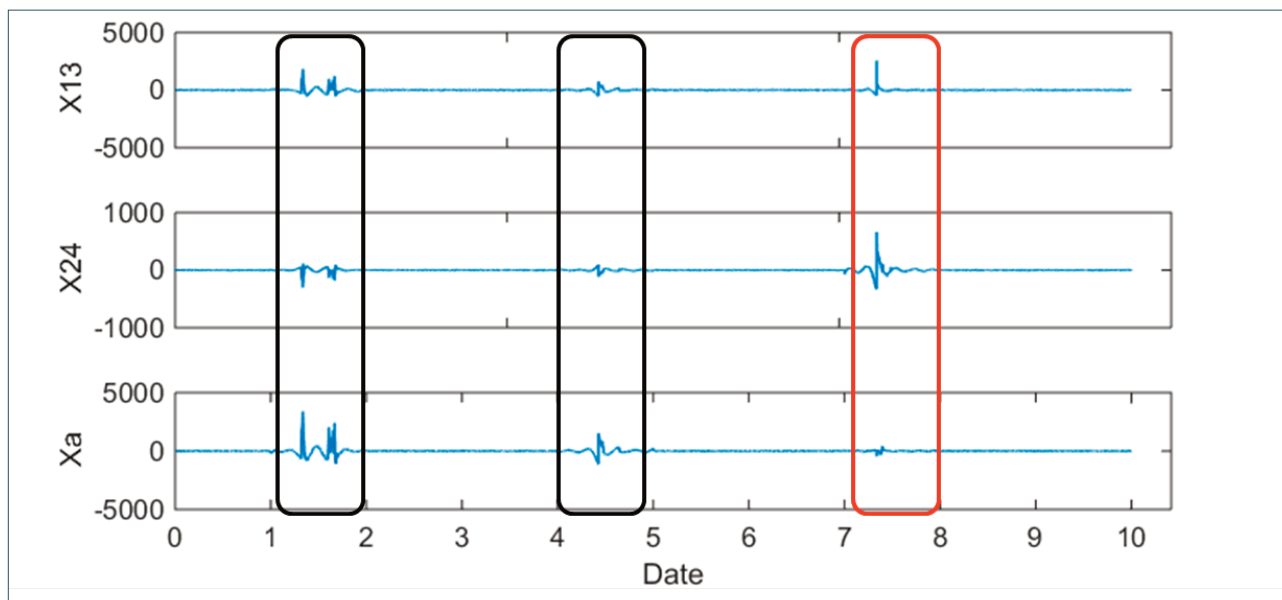


FIGURE 3. Synthetic signals: X_{13} , X_{24} and X_a . Black box represents precursory anomaly signals, and red box represents coseismic signal.

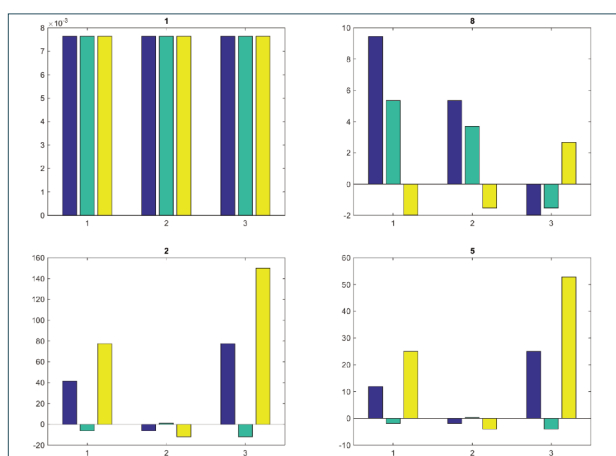


FIGURE 4. The covariance matrices of the standard days and the anomalous days.

anomaly signals.

Here the eigenvectors represent the spatial distribution information of covariance matrix, and the eigenvalues represent the amplitude information of covariance matrix. From the results of synthetic data, PCA has the ability to detect such precursory abnormal signals.

3.3 DATA PROCESSING

PCA is applied to extract the anomalies of strain changes associated with the earthquake. We analyse the borehole strain data from the Guza Station that were collected from January 01 2011, to December 31, 2013. Figure 6 shows the four-component series of borehole strain data that were recorded at the Guza Station.

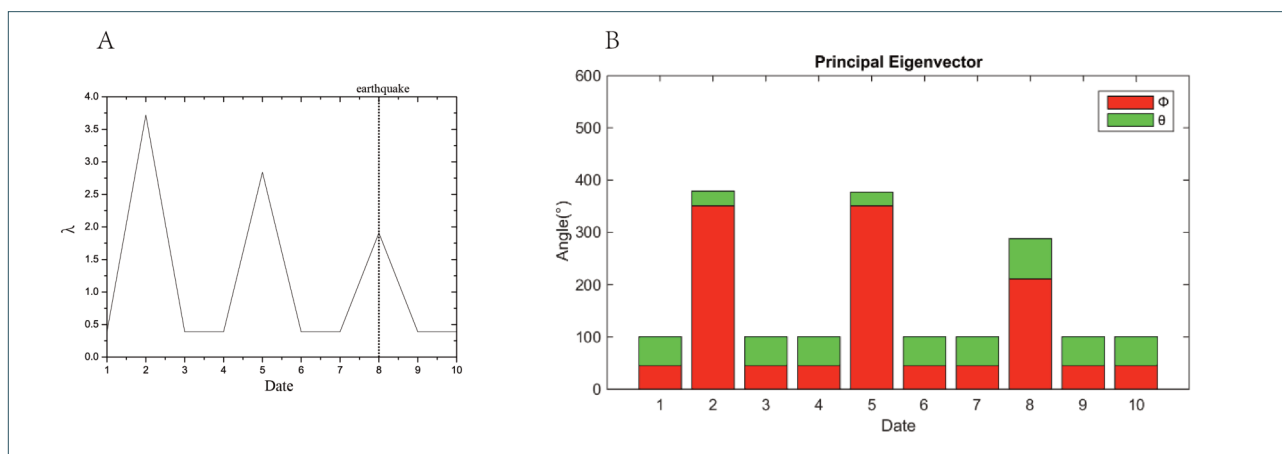


FIGURE 5. The results of the daily variations in the first principal component eigenvalue (A), and the histogram of the θ and ϕ angles (B).

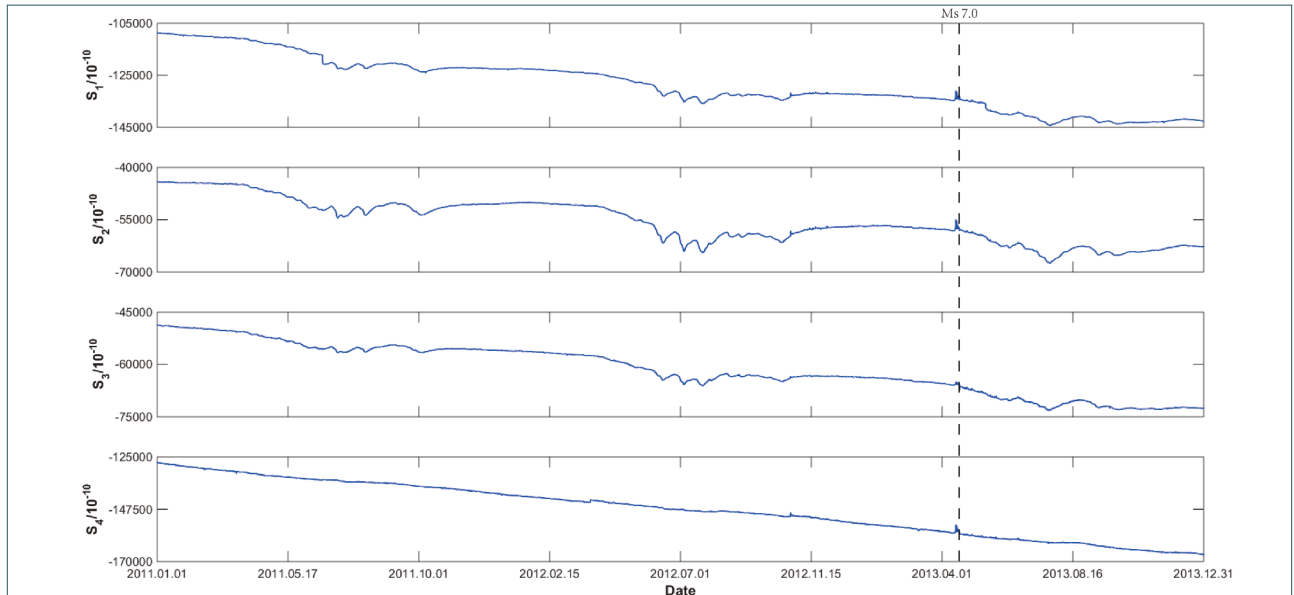


FIGURE 6. The four-component time series of borehole strain data recorded at the Guza Station, China, from January 01, 2011, to December 31, 2013.

First, the borehole strain data from the Guza Station are checked using the self-consistency equation, after which the four-component borehole strain data are transformed into three components, namely, S_{13} , S_{24} , and S_a , through a strain conversion. The next step is data preprocessing, in which we remove the influences of solid tide and the trend reflecting seasonal variation by using a harmonic analysis. The strain changes that reflect the movements of the crust that are associated with the earthquake are regarded as the short period high frequency oscillation signal. The information regarding the strain change that is related to crustal activity is the most dominant signal in the daily variation data.

Surrounding environment of the station is one of the factors affecting borehole strain data. Most of these factors have a cycle of one day. In order to avoid time-domain aliasing, and distinguish the anomalous days easier, we chose to perform PCA on daily data. Let us consider that the three-component data (i.e., 1 day is equal to 1440 points) are arranged in the form of time series data vectors.

$$\begin{cases} \mathbf{S}_{13} = [\mathbf{S}_{13}(t_1), \mathbf{S}_{13}(t_2), \dots, \mathbf{S}_{13}(t_{1440})]^T \\ \mathbf{S}_{24} = [\mathbf{S}_{24}(t_1), \mathbf{S}_{24}(t_2), \dots, \mathbf{S}_{24}(t_{1440})]^T \\ \mathbf{S}_a = [\mathbf{S}_a(t_1), \mathbf{S}_a(t_2), \dots, \mathbf{S}_a(t_{1440})]^T \end{cases} \quad (5)$$

where T indicates a transpose. Then, the data matrix $\mathbf{Y} = [\mathbf{S}_{13}, \mathbf{S}_{24}, \mathbf{S}_a]^T$ is prepared. A time-series plot of the borehole strain data after the strain conversion are shown in Figure 7 and the data after data preprocessing are shown in Figure 8.

The co-variance matrix that consists of borehole

strain data after the strain conversion \mathbf{C}_Y is then computed. The eigenvalue decomposition of \mathbf{C}_Y is performed to obtain $\mathbf{C}_Y = \mathbf{V}\mathbf{\Lambda}\mathbf{V}^T$, where $\mathbf{\Lambda}$ is the eigenvalue matrix consisting of the eigenvalues $\lambda_1, \lambda_2, \lambda_3$ ($\lambda_1 > \lambda_2 > \lambda_3$) and \mathbf{V} is the eigenvector matrix with v_1, v_2, v_3 . In the PCA approach the eigenvector v_1 is chosen to maximize the variance in the data. We consider that the eigenvector v_1 is the most intense signal subspace [Hattori et al., 2004]. Since we previously transformed the data into three components, it is possible to perform an orthogonal expansion of the signal space into v_2 and v_3 which are the second and third principal components, respectively.

4. RESULTS AND DISCUSSIONS

Through a field investigation and a comparison of the correlations among strain data and seismographic recordings, Qiu et al. [2013b] concluded that the abnormal changes observed at the Guza Station (several days before the earthquake) should be related to the Lushan earthquake. Chi et al. [2013] also observed abnormal strain five months before the Lushan earthquake that lasted for 3 months. Based on the results of these previous studies, we conduct the following investigation.

We apply PCA to the data after pretreatment, and calculate the first principal component eigenvalue and eigenvector. Figure 9 shows the daily variation in the first principal component eigenvalue λ . The earthquake occurrence is shown with a vertical dashed line. We calculate the average and the standard deviation σ using

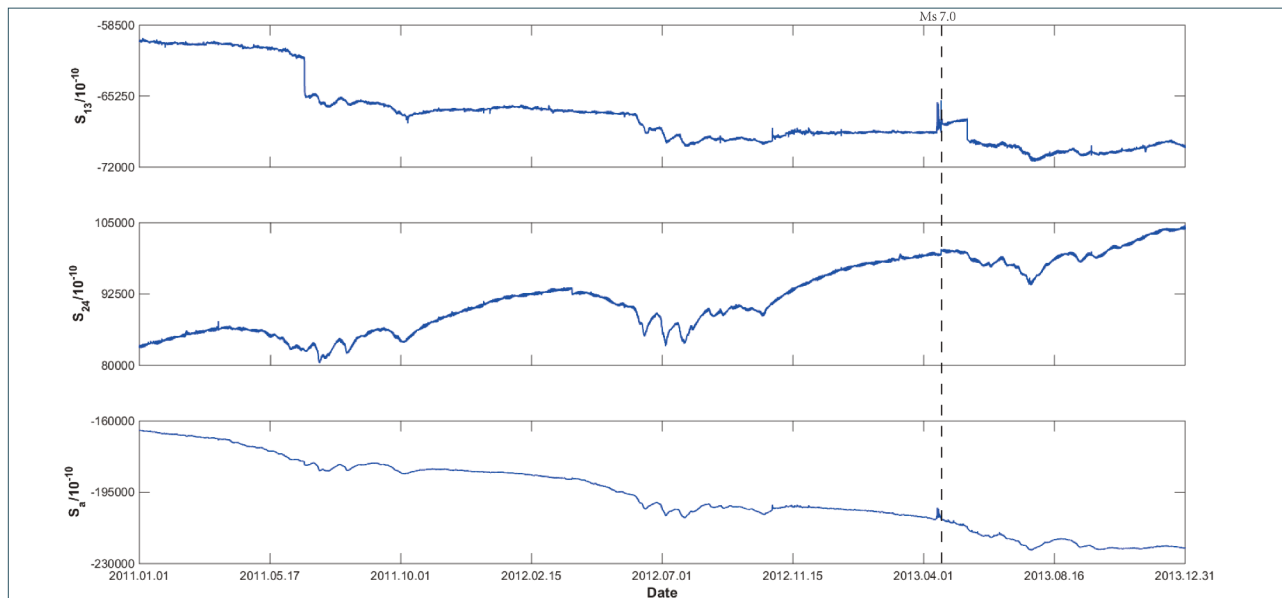


FIGURE 7. A time series plot of borehole strain data after the strain conversion. S_{13} and S_{24} represent the two independent shear strains, and S_a represents the areal strain.

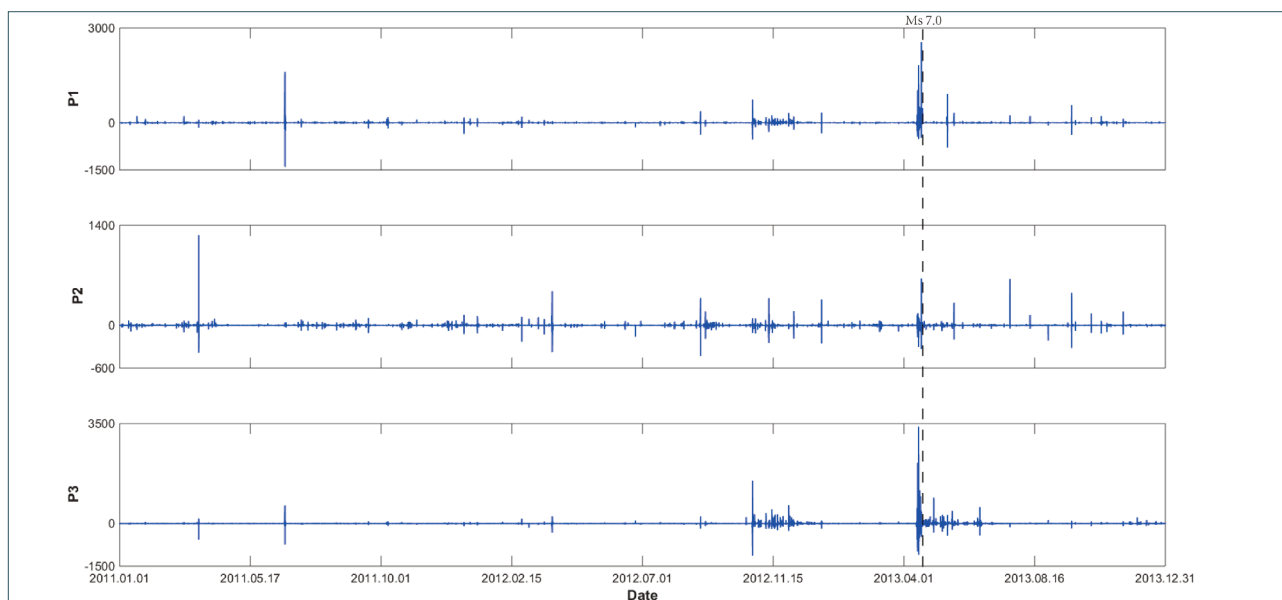


FIGURE 8. A time series plot of data after data preprocessing. P1, P2 and P3 represent the data after data preprocessing of S_{13} , S_{24} and S_a , respectively.

all of the values to recognize anomalous λ values. Those anomalous values are then defined as values that exceed the average by more than 1σ .

The variations in λ that are shown in Figure 9 illustrate that the anomalous values are mainly concentrated in two time periods, October 25–December 30, 2012 and April 15–19, 2013, the latter of which was just several days before the earthquake occurred. These results are consistent with those of Qiu et al. [2013b] and Chi et al. [2013]. In addition, the anomalous values also appeared on January 28, 2011; March 24, 2011; June 23, 2011;

October 7, 2011; October 9, 2011; March 29, 2012; August 31, 2012 before the Lushan earthquake. Figure 9 indicates that the anomaly that occurred during the period of April 15–19, 2013, has an adequate correlation with the Lushan earthquake. However, it seems that there is no correlation between the two abnormal time periods.

To study the relationship between these two partial anomalies, we analyse the corresponding eigenvectors. Since the number of PCA dimensions is three, the eigenvectors obtained have the same numbers of dimensions

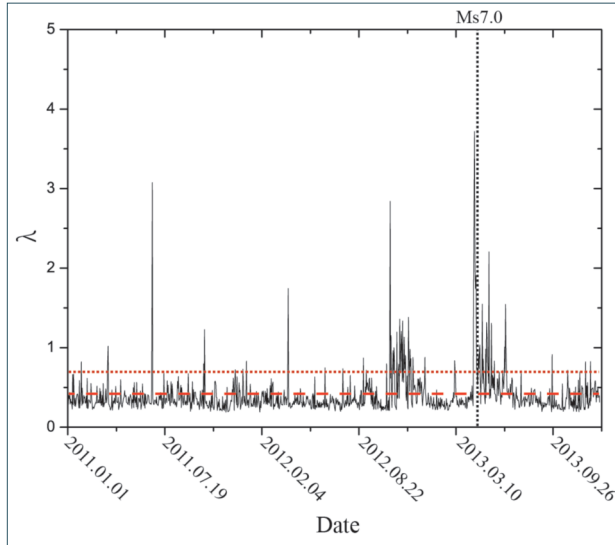


FIGURE 9. The results of the daily variations in the first principal component eigenvalue. The average value is delimited by a red horizontal dashed line, and the average of more than 1σ is delimited by a red horizontal dotted line.

the signal subspace. And the covariance matrices of a few standard days and a few anomalous days have been showed in Figure 11. Covariance matrices of standard days show the random characteristics, and those of anomalous days show the similar distribution. It is significant that the main anomalous behaviour that precedes the earthquake shares the same signal pattern.

We take the eigenvector for the anomalous days preceding the earthquake as the abnormal eigenvector, and a similarity measurement based on the distance is applied to extract other abnormal eigenvectors using equation (6):

$$d = \sqrt{(\theta - \theta_i)^2 + (\phi - \phi_i)^2}, \quad i = 1, 2, \dots, n \quad (6)$$

where θ and ϕ are the average angles of the eigenvector for the anomalous days preceding the earthquake, and θ_i and ϕ_i are the angles of the eigenvector for the days to be measured. We observe that when $0 \leq d \leq 15$, the extracted anomalies are most trusted, and we treat

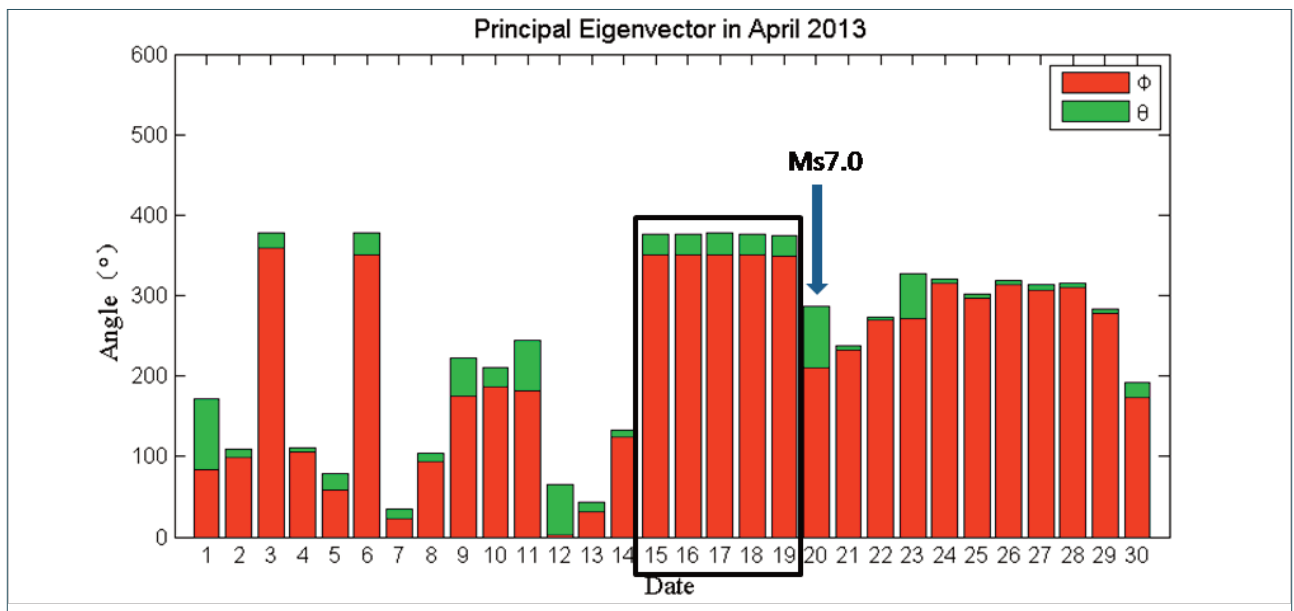


FIGURE 10. The histogram of the θ and ϕ angles for April, 2013. The black box marks suspected abnormal days, and the blue arrow denotes the day of the earthquake.

in the vector space. To express the eigenvectors more intuitively, we consider a two-dimensional plot with the angles θ and ϕ . The eigenvector shows the basis function of a signal subspace.

First, we study the eigenvector for the several days preceding the earthquake. Figure 10 illustrates the daily variations in the eigenvector for April 2013; we find that the anomalies during the period of April 15-19 show a similar distribution in both θ and ϕ . This indicates that these days possess the same basis function of

them as targets.

Figure 12 indicates the results of the detection of abnormal eigenvectors over the analysed period. A large number of abnormal eigenvectors similar to those preceding the earthquake are observed during from October 2012 to January 2013. The two anomalous periods detected from the variations in the eigenvalues show a strong correlation among the eigenvectors. Similar eigenvector distributions do not appear on January 28, 2011; March 24, 2011; June 23, 2011; October 7, 2011;

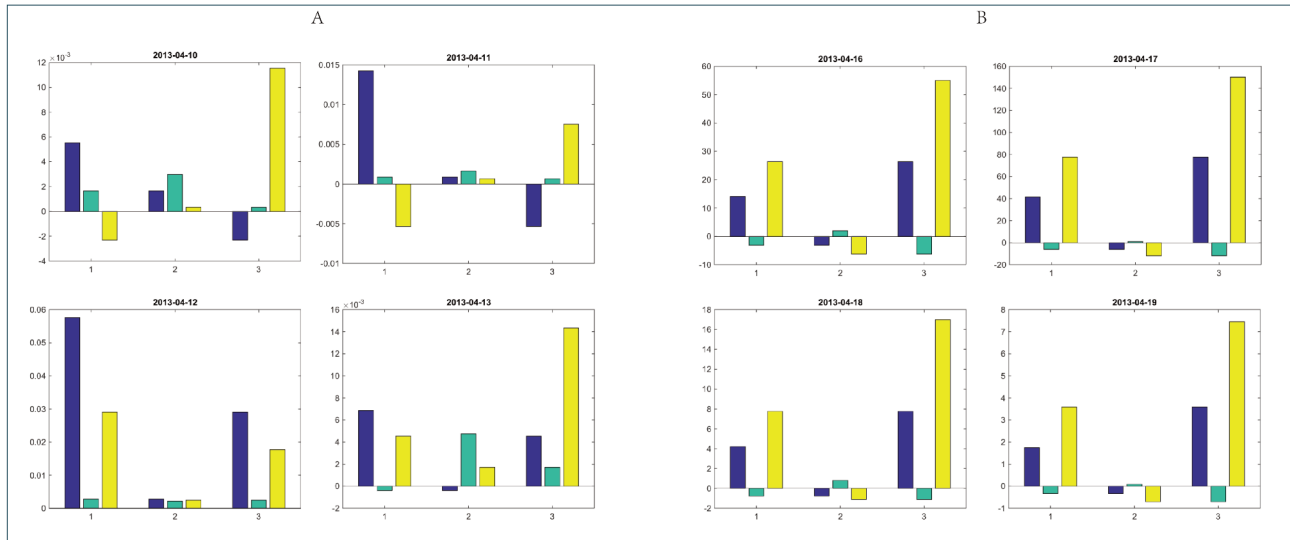


FIGURE 11. The covariance matrices of a few standard days and a few anomalous days. A is the covariance matrices of a few standard days; B is the covariance matrices of a few anomalous days.



FIGURE 12. The results of the detection of abnormal eigenvectors from January 2011 to December 2013. The black boxes mark suspected abnormal eigenvectors, and the blue arrow denotes the day of the earthquake.

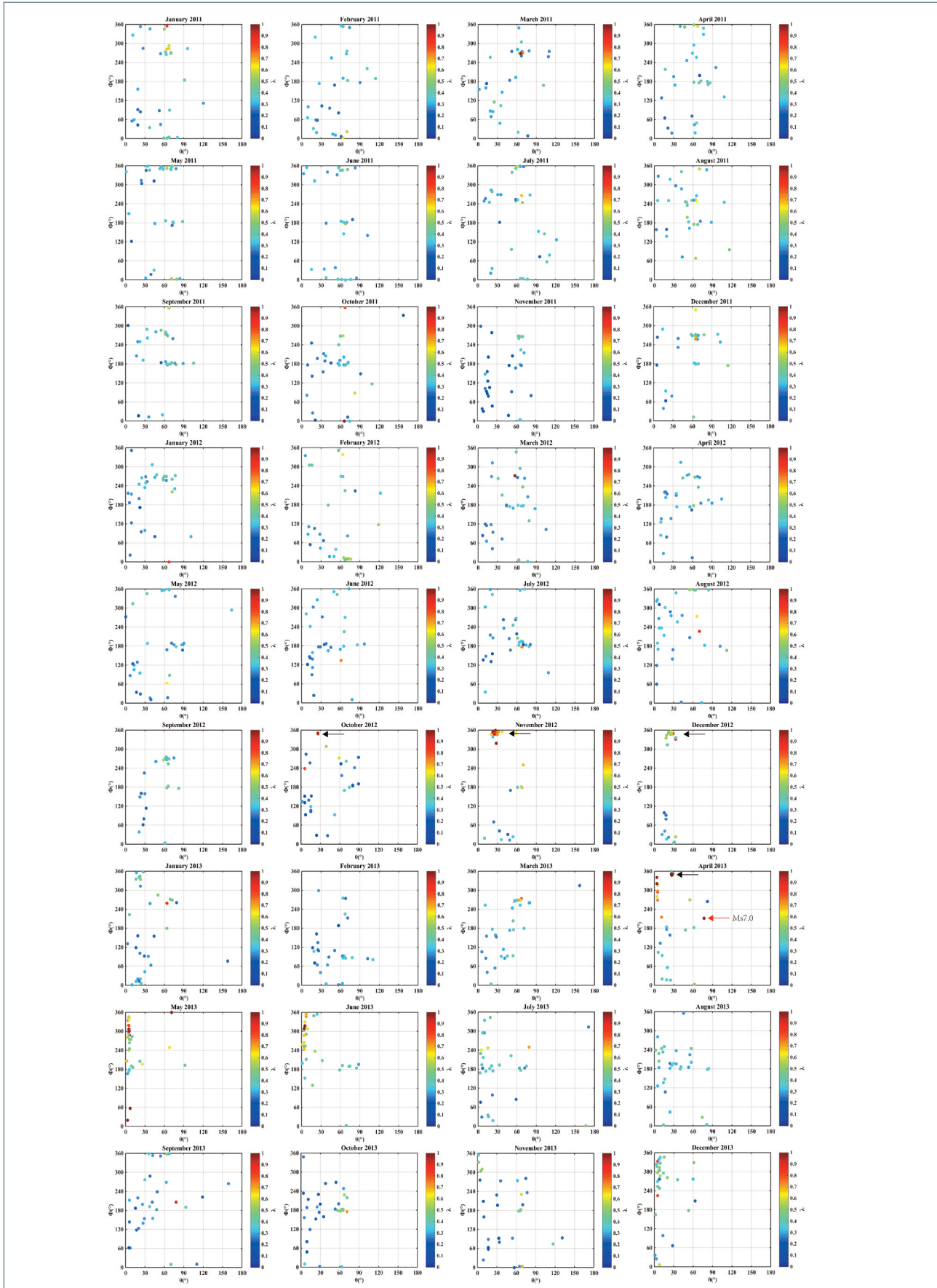


FIGURE 13. The result of the spatial distribution of eigenvalues and eigenvectors. The x-axis and y-axis respectively represent the λ and ϕ angles, ϕ and the colour indicates the changes in eigenvalue. The black arrow denotes the suspected abnormal days, and the red arrow denotes the day of the Lushan earthquake.

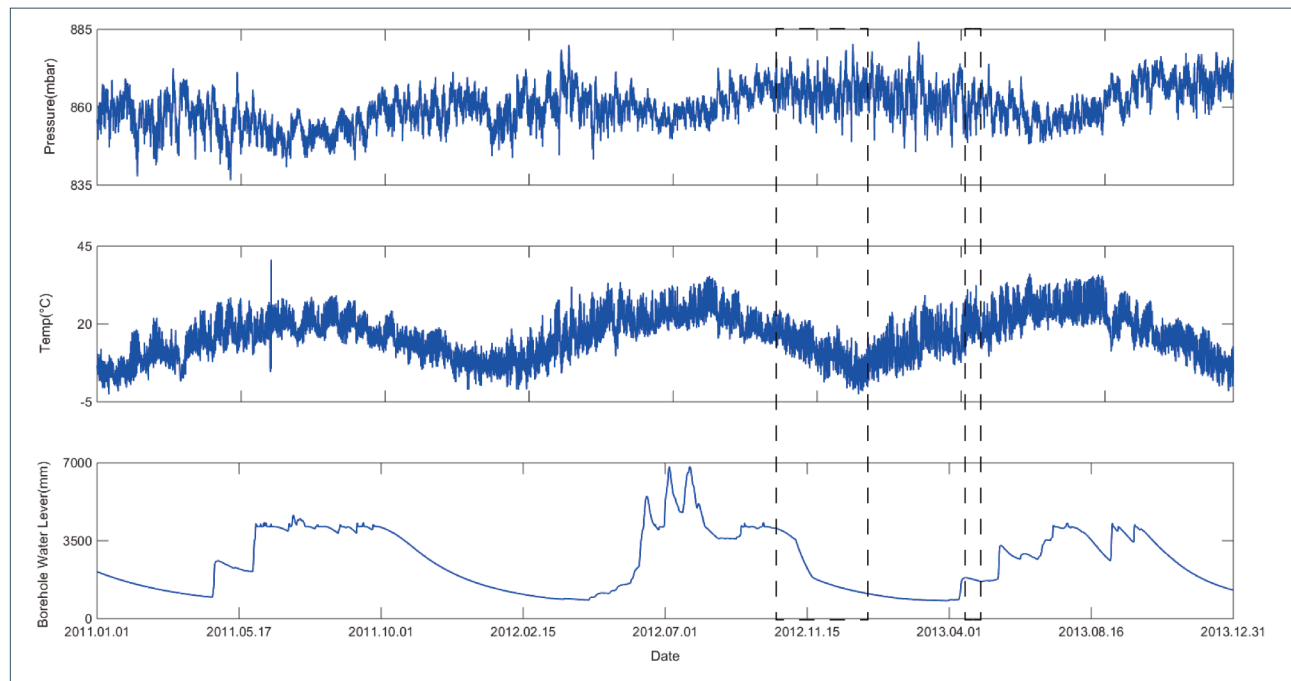


FIGURE 14. Pressure data (upper panel), temperature data (middle panel), borehole water lever data (lower panel) of Guza station, during January 01, 2011 to December 31, 2013.

October 9, 2011; March 29, 2012; August 31, 2012.

Here, we must mention that the results of the anomaly detection using the eigenvalue and those obtained using eigenvector are not exactly the same. We consider that the eigenvalue and eigenvector are both obtained from the decomposition of the co-variance matrix of the data and that both contain parts of information of the data.

To avoid the loss of information and to extract the data anomalies more accurately, we perform a combined eigenvalue and eigenvector analysis. Figure 13 shows the spatial distributions of eigenvalues and eigenvectors. During the periods of October 25–December 30, 2012, and April 15–19, 2013, the abnormal days show a clustered distribution (black arrow), in the same location. Other days are scattered irregularly throughout the spatial coordinate system.

Time series plot of factors that affect soil radon activity is shown in Figure 14. This displays pressure variation, temperature variation, and borehole water lever variation during the observation period. To some extent, the borehole water level reflects the change of rainfall. The black dashed boxes corresponds to the periods of the two part of abnormal. As is shown in Figure 13, pressure variation and temperature variation did not show abnormal phenomena in the periods of the two part of abnormal. The periods of the two part of abnormal are in the dry season of this region, and borehole water lever shows the downward trend. It can basically be ruled out that anomalies are caused by pressure, temperature, and the rainfall.

Based upon the results from the combined eigenvalue

and eigenvector analysis, the spatial distribution of the pre-earthquake anomaly is very similar to the distributions of eigenvectors and eigenvalues for the period from October 2012 to December 2012 that precedes the earthquake. We infer that a similar process contributed to the formation of both anomalies and that these two anomalies are both earthquake precursors associated with the Lushan earthquake.

5. CONCLUSION

We have utilized the eigenvalues and eigenvectors of the first principal component of time series borehole strain data using PCA technique to study the abnormal characteristics of borehole strain data that preceded the Lushan earthquake. PCA is capable of effectively extracting abnormal features. This application of PCA to investigate on strain earthquake precursors is still in an embryonic stage. There are many problems that must yet be resolved. Because the principle of crustal movement is complex, it is difficult to determine the physical meaning of eigenvalues and eigenvectors, and because of the different observation principles and accuracy of different types of strain data, it is difficult to use a PCA method with this information to carry out a joint analysis. However, by applying PCA to describe the strain behaviour, we may be able to ensure that the PCA technique has great potential in the study of earthquake precursors.

Acknowledgements. The authors are grateful to the Key Laboratory of the Geo-Exploration Instrumentation of Ministry of Education in Jilin University of China. Moreover, the authors are appreciative of Professor Xiuying Wang and Professor Zehua Qiu for their help and valuable suggestions. This research was supported by the Institute of Crustal Dynamics, China Earthquake Administration (Grant No.3R216N620537).

REFERENCES

- Asai Y., Okubo M., Ishii H., et al (2005). Co-seismic strain-steps associated with the 2004 off the Kii peninsula earthquakes—Observed with Ishii-type borehole strainmeters and quartz-tube extensometers. *J. Earth, planets and space*. 57(4): 309–314.
- Barbour A.J., Agnew D.C (2012). Detection of seismic signals using seismometers and strainmeters. *J. Bulletin of the Seismological Society of America*. 102(6): 2484–2490.
- Chi S L., Liu Q., Chi Y., et al (2013). Borehole strain anomalies before the 20 April 2013 Lushan Ms 7.0 earthquake. *J. Acta Seismol Sin.* 35(3): 296–303.
- C. Goltz (2001). Decomposing spatio-temporal seismicity patterns. *J. Natural Hazards and Earth System Science, Copernicus Publications on behalf of the European Geosciences Union*. 1 (1/2). pp.83–92. <hal-00298988>.
- Fang Y, Jing, Z., Zai-Sen, J., Zhi-Gang, S., & Jian-Ling, C. (2015). Movement characteristics of the northwest segment of the Xianshuihe fault zone derived from cross-fault deformation data. *CHINESE JOURNAL OF GEOPHYSICS-CHINESE EDITION*, 58(5), 1645–1653.
- Gómez Londoño E., Castillo López L., Thaís de Souza K (2005). Using the Karhunen-Loeve transform to suppress ground roll in seismic data. *J. Earth Sciences Research Journal*. 9(2): 139–147.
- Gotoh K., Akinaga Y., Hayakawa M., et al (2003). Principal component analysis of ULF geomagnetic data for Izu islands earthquakes in July 2000. *EGS-AGU-EUG Joint Assembly*.
- Hattori K., Serita A., Gotoh K., et al. (2004). ULF geomagnetic anomaly associated with 2000 Izu islands earthquake swarm, Japan. *J. Physics and Chemistry of the Earth, Parts A/B/C*. 29(4): 425–435.
- Hattori K., Han P., Huang Q (2013). Global variation of ULF geomagnetic fields and detection of anomalous changes at a certain observatory using reference data. *J. Electrical Engineering in Japan*. 182(3): 9–18.
- Hautmann. S., D. Hidayat., N. Fournier., A. T. Linde., I. S. Sacks., and C. P. Williams (2013). Pressure changes in the magmatic system during the December 2008/January 2009 extrusion event at Soufriere Hills Volcano, Montserrat (W.I.), derived from strain data analysis. *J. Volcanol. Geotherm. Res.* 250, 34–41.
- Johnston M.J.S., Linde A.T., Agnew D.C (1994). Continuous borehole strain in the San Andreas fault zone before, during, and after the 28 June 1992, Mw 7.3 Landers, California, earthquake. *J. Bulletin of the Seismological Society of America*. 84(3): 799–805.
- Johnston M.J.S., Borchardt R D., Linde A T., et al (2006). Continuous borehole strain and pore pressure in the near field of the 28 September 2004 M 6.0 Parkfield, California, earthquake: Implications for nucleation, fault response, earthquake prediction, and tremor. *J. Bulletin of the Seismological Society of America*. 96(4B): S56–S72.
- Lin Jyh-Woei (2011). Use of principal component analysis in the identification of the spatial pattern of an ionospheric total electron content anomalies after China’s May 12, 2008, M= 7.9 Wenchuan earthquake. *J. Advances in Space Research*. 47(11): 1983–1989.
- Liu C.C., Linde A.T., Sacks I.S (2009). Slow earthquakes triggered by typhoons. *J. Nature*. 459(7248): 833–836.
- Linde, A. T., M. T. Gladwin., M. J. S. Johnston., R. L. Gwyther and R. G. Bilham (1996). A slow earthquake sequence on the San Andreas fault. *J. Nature*. 383. 65–68.
- McGarr A., Sacks I.S., Linde A.T., et al (1982). Coseismic and other short-term strain changes recorded with Sacks-Evertson strainmeters in a deep mine, South Africa. *J. Geophysical Journal International*. 70(3): 717–740.
- Ouyang Z.X., Zhang H.X., Fu Z.Z., et al (2009). Abnormal phenomena recorded by several earthquake precursor observation instruments before the Ms 8.0 Wenchuan, Sichuan earthquake. *J. Acta Geologica Sinica (English Edition)*. 83(4): 834–844.
- Qi L., Jing Z (2011). APPLICATION OF S TRANSFORM IN ANALYSIS OF STRAIN CHANGES BEFORE AND AFTER WENCHUAN EARTHQUAKE. *J. Journal of Geodesy and Geodynamics*. 4: 003.
- Qiu Z.H., Zhang B., Huang X., et al (1998). On the cause of ground stress tensile pulses observed before the 1976 Tangshan earthquake. *J. Bulletin of the Seismological Society of America*. 88(4): 989–994.
- Qiu Z.H., Shi Y (2003). Observations of remote coseismic stress step-changes. *J. Science in China Series D: Earth Sciences*. 46: 75–81.
- Qiu Z.H., Shi Y (2004). Application of observed strain steps to the study of remote earthquake stress triggering. *J. Earthquake Science*. 17(5): 534.
- Qiu Z.H., Zhang B H., Chi S L., et al (2011). Abnormal

- strain changes observed at Guza before the Wenchuan earthquake. *J. Science China Earth Sciences*. 54(2): 233-240.
- Qiu Z.H., Tang L., Zhang B., et al (2013a). In situ calibration of and algorithm for strain monitoring using four gauge borehole strainmeters (FGBS). *J. Journal of Geophysical Research: Solid Earth*. 118(4): 1609-1618.
- Qiu Z.H., Guang Y., Lei T., et al (2013b). Abnormal strain changes observed by a borehole strainmeter at Guza Station before the Ms7.0 Lushan earthquake. *J. Geodesy and Geodynamics*. 4(3): 19-29.
- Qiu Z.H., Chi S., Wang Z., et al (2015). The strain seismograms of P-and S-waves of a local event recorded by four-gauge borehole strainmeter. *J. Earthquake Science*. 28(3): 209-214.
- Sacks, I. S., S. Suyehiro., A. T. Linde and J. A. Snoke (1978). Slow earthquakes and stress redistribution. *J. Nature*. 275, 599-602.
- Sacks, I. S., Linde, A. T., Snoke, J. A., & Suyehiro, S (1981). A Slow Earthquake Sequence Following the Izu Oshima Earthquake of 1978. *J. Earthquake Prediction*, 617-628.
- Sturkell, E., K. Agustsson, A.T. Linde, S.I. Sacks, P. Einarsson, F. Sigmundsson, H. Geirsson, R. Pedersen, P.C. La Femina and H.Olafsson (2013). New insights into volcanic activity from strain and other deformation data for the Hekla 2000 eruption. *J. Volcanol. Geotherm. Res.* 256, 78-86.
- Telesca L., Colangelo G., Hattori K., et al (2004). Principal component analysis of geoelectrical signals measured in the seismically active area of Basilicata Region (southern Italy). *J. Natural Hazards and Earth System Sciences*. 4(5/6): 663-667.
- Voight, B., et al (2006). Unprecedented pressure increase in deep magma reservoir triggered by lava-dome collapse. *J. Geophys. Res. Lett.* 33,L03312, doi:10.1029/2005GL024870.
- Zeng X F Luo Y Han L B et al (2013) The Lushan Ms7.0 earthquake on 20 April 2013 A high angle thrust event. *Chinese J. Geophys.* (in Chinese). 56(4) 1418-1424 doi 10.6038/cjg20130437.

*CORRESPONDING AUTHOR: Kaiguang ZHU,
Key Laboratory of Geo-Exploration Instrumentation,
Ministry of Education, Jilin University,
Changchun, People's Republic of China

email: zhukaiguang@jlu.edu.cn